Available online at www.sciencedirect.com
SCIENCE DIRECT®
Journal of Magnetic Resonance 169 (2004) 49–59
JMR Journal of Magnetic Resonance
www.elsevier.com/locate/jmr

Determining the relative sign and size of scalar and residual dipolar couplings in homonuclear two-spin systems

Frank Kramer,[a] Astrid Jung,[b] Eike Brunner,[b] and Steffen J. Glaser[a,*]

[a] *Department Chemie, Technische Universität München, Lichtenbergstr. 4, D-85747 Garching, Germany*
[b] *Institute of Biophysics and Physical Biochemistry, University of Regensburg, D-93040 Regensburg, Germany*

Received 2 March 2004; revised 31 March 2004
Available online 5 May 2004

Abstract

Based on the sign and amplitude of TOCSY transfer functions, it is possible to determine the relative sign and size of scalar and residual dipolar couplings in homonuclear spin systems consisting of two spins 1/2. The efficiency of different mixing sequences and different transfer functions is examined both theoretically and experimentally.

Keywords: Hartmann–Hahn transfer; Residual dipolar couplings; Dipolar mixing; TOCSY

1. Introduction

In the weak coupling limit, the spectrum of two scalarly and dipolarly coupled spins does not allow to unequivocally determine the relative sign and size of scalar and residual dipolar coupling constants. One solution to the problem is to use an additional spin to solve the sign ambiguity [1]. Alternatively, the preparation of several samples with different degrees of alignment allows to solve the sign problem. Here we present a different approach, which allows to solve the sign problem for a pair of homonuclear spins in a single aligned sample if the scalar coupling is known. The method relies on the fact that TOCSY transfer functions reflect the full scalar and dipolar coupling tensors. This makes it possible to determine the sign of residual dipolar couplings in the presence of known scalar couplings in a two-spin system. The approach is demonstrated experimentally using a model system and potential problems of the approach are discussed.

2. Theory

We consider a system consisting of two homonuclear spins 1/2 termed I and S. In the presence of both dipolar and scalar couplings the coupling Hamiltonian has the form:

$$\mathsf{H}_C = \mathsf{H}_D + \mathsf{H}_J \tag{1}$$

with the dipolar coupling term

$$\mathsf{H}_D = 2\pi D\left\{I_{1z}I_{2z} - \tfrac{1}{2}I_{1x}I_{2x} - \tfrac{1}{2}I_{1y}I_{2y}\right\}, \tag{2}$$

and the scalar coupling term

$$\mathsf{H}_J = 2\pi J\left\{I_{1z}I_{2z} + I_{1x}I_{2x} + I_{1y}I_{2y}\right\}. \tag{3}$$

Hence, the total coupling term H_C is given by

$$\begin{aligned}\mathsf{H}_C &= 2\pi\left\{(D+J)I_{1z}I_{2z} + (J-D/2)(I_{1x}I_{2x} + I_{1y}I_{2y})\right\}\\ &= 2\pi\left\{C^L I_{1z}I_{2z} + C^P(I_{1x}I_{2x} + I_{1y}I_{2y})\right\}\end{aligned} \tag{4}$$

with $C^L = D + J$ and $C^P = J - D/2$. In the weak coupling limit, the observed splitting Δ is given by the absolute value of the sum of J and D:

$$\Delta = |C^L| = |D + J|. \tag{5}$$

Hence a given splitting Δ can result from $C^L = \Delta = D^{(+)} + J$ or $C^L = -\Delta = D^{(-)} + J$, with the two possible dipolar coupling constants

$$D^{(+)} = \Delta - J \tag{6}$$

* Corresponding author. Fax: +49-89-289-13210.
E-mail address: glaser@ch.tum.de (S.J. Glaser).

1090-7807/$ - see front matter © 2004 Elsevier Inc. All rights reserved.
doi:10.1016/j.jmr.2004.04.002

or

$$D^{(-)} = -\Delta - J. \tag{7}$$

For example, for a scalar coupling of $J = 7\,\mathrm{Hz}$, an observed splitting of $\Delta = 3.5$ Hz can either result from a dipolar coupling $D^{(+)} = -3.5\,\mathrm{Hz}$ or from a dipolar coupling $D^{(-)} = -10.5\,\mathrm{Hz}$. These two cases cannot be distinguished for a two-spin system in the weak coupling limit.

Now we consider a TOCSY sequence [2–4] which creates the following average coupling terms for two on-resonance spins [5]:

$$\overline{\mathsf{H}_D} = 2\pi\bar{D}\left\{I_{1z'}I_{2z'} - \tfrac{1}{2}I_{1x'}I_{2x'} - \tfrac{1}{2}I_{1y'}I_{2y'}\right\} \tag{8}$$

and

$$\overline{\mathsf{H}_J} = \mathsf{H}_J. \tag{9}$$

Hence

$$\begin{aligned}\overline{\mathsf{H}_C} &= \overline{\mathsf{H}_D} + \overline{\mathsf{H}_J} \\ &= 2\pi\left\{\overline{C^L}I_{1z'}I_{2z'} + \overline{C^P}\left(I_{1x'}I_{2x'} + I_{1y'}I_{2y'}\right)\right\},\end{aligned} \tag{10}$$

where

$$\overline{C^L} = J + \bar{D} = J + sD \tag{11}$$

is the effective longitudinal coupling constant,

$$\overline{C^P} = J - \tfrac{1}{2}\bar{D} = J - sD/2 \tag{12}$$

is the effective transverse coupling constant and

$$s = \bar{D}/D \tag{13}$$

is the dipolar scaling factor [5]. In the principal axis system (x', y', z') of the effective coupling tensor [6], the transverse and longitudinal transfer functions $T_{x'} = T_{y'}$ and $T_{z'}$ are given by

$$\begin{aligned}T_{x'} = T_{y'} &= \sin(\pi\overline{C^P}\tau)\sin(\pi\overline{C^L}\tau) \\ &= \sin(\pi\{J - sD/2\}\tau)\sin(\pi\{J + sD\}\tau)\end{aligned} \tag{14}$$

and

$$T_{z'} = \sin^2(\pi\overline{C^P}\tau) = \sin^2(\pi\{J - sD/2\}\tau). \tag{15}$$

For the two possible values ($D^{(+)}$ and $D^{(-)}$, cf. Eqs. (6) and (7)) of the dipolar coupling constant D, Eqs. (14) and (15) can be rewritten as

$$\begin{aligned}T_{x'}^{(\pm)} = T_{y'}^{(\pm)} &= \sin(\pi\{J - sD^{(\pm)}/2\}\tau)\sin(\pi\{J + sD^{(\pm)}\}\tau) \\ &= \sin(\pi\{(1 + s/2)J \mp s\Delta/2\}\tau)\sin(\pi\{(1 - s)J \pm s\Delta\}\tau)\end{aligned} \tag{16}$$

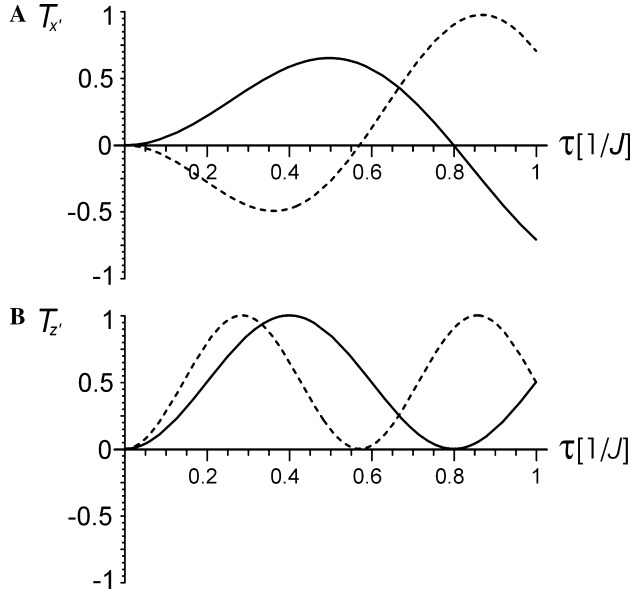

Fig. 1. Time-dependence of the transfer functions $T_{x'}^{(+)}$ (solid curve) and $T_{x'}^{(-)}$ (dashed curve) (A) and $T_{z'}^{(+)}$ (solid curve) and $T_{z'}^{(-)}$ (dashed curve) (B) for the dipolar scaling factor $s = 1$ and a line splitting $\Delta = |J|/2$.

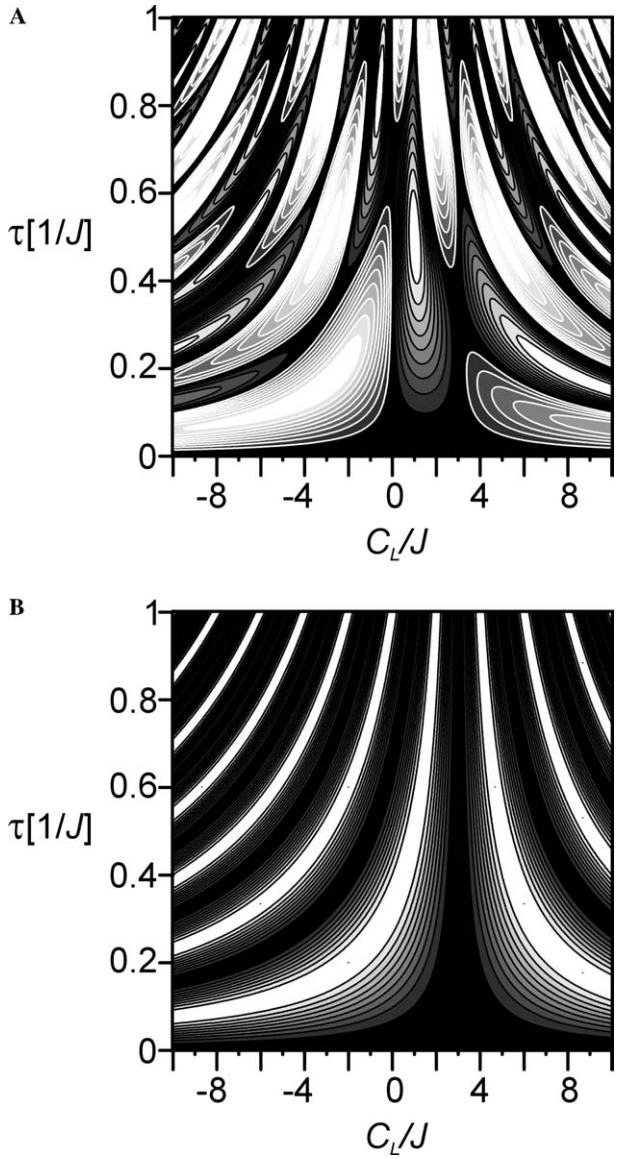

Fig. 2. Time dependence of the transfer functions $T_{x'}(\tau)$ (A) and $T_{z'}(\tau)$ (B) for different ratios C_L/J and a dipolar scaling factor $s = 1$.

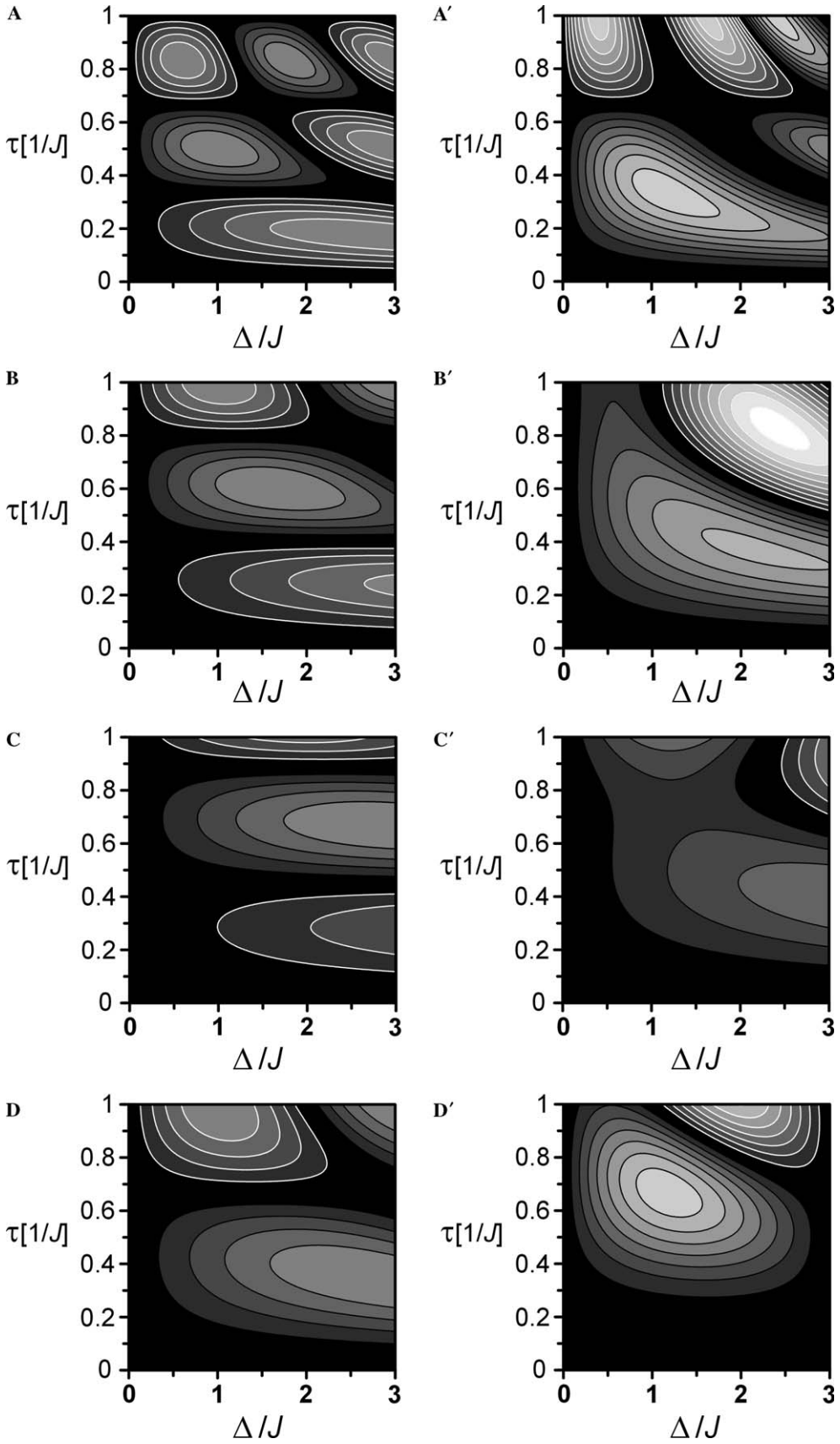

Fig. 3. Differences $T^{(+)}_{\alpha'} - T^{(-)}_{\alpha'}$ between the transverse ($\alpha = \{x' \text{ or } y'\}$ see A–D) and longitudinal ($\alpha = z'$ see A′–D′) transfer functions for $s = 1$ (A, A′), $s = 0.5$ (B, B′), $s = 0.25$ (C, C′), and $s = -0.5$ (D, D′). Contour lines (black if positive, white if negative) are shown for $\pm 0.2, \pm 0.4, \ldots$ Areas with the same value $T^{(+)}_{\alpha'} - T^{(-)}_{\alpha'}$ are filled with the same grey level (e.g., black for $|T^{(+)}_{\alpha'} - T^{(-)}_{\alpha'}| \leqslant 0.2$).

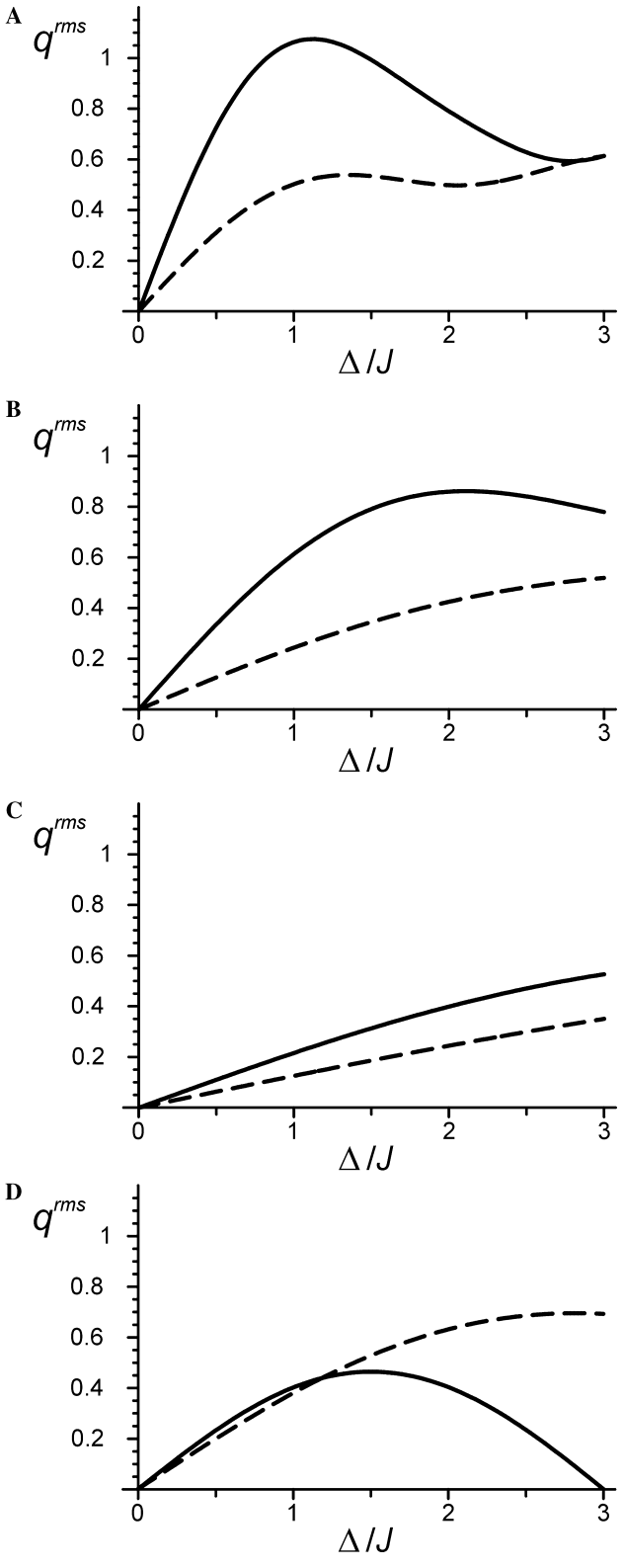

Fig. 4. Root mean square difference q^{rms} of transverse (solid curves) and longitudinal (dashed curves) transfer for $0 \leqslant \tau \leqslant 1/J$ (cf. Eq. (21)) and the dipolar scaling factors $s = 1$ (A), $s = 0.5$ (B), $s = 0.25$ (C), and $s = -0.5$ (D).

and

$$\begin{aligned} T_{z'}^{(\pm)} &= \sin^2(\pi\{J - sD^{(\pm)}/2\}\tau) \\ &= \sin^2(\pi\{J - s(\pm\Delta - J)/2\}\tau) \\ &= \sin^2(\pi\{(1 + s/2)J \mp s\Delta/2\}\tau). \end{aligned} \tag{17}$$

In general, the transfer functions $T_{x'}^{(+)}$ (or $T_{z'}^{(+)}$) are different from the transfer functions $T_{x'}^{(-)}$ (or $T_{z'}^{(-)}$). For the ideal case where the scaling factor s approaches 1, the transfer functions simplify to

$$T_{x'}^{(\pm)} = T_{y'}^{(\pm)} = \pm \sin(\tfrac{\pi}{2}(3J \mp \Delta)\tau)\sin(\pi\Delta\tau) \tag{18}$$

and

$$T_{z'}^{(\pm)} = \sin^2(\tfrac{\pi}{2}(3J \mp \Delta)\tau). \tag{19}$$

Fig. 1 shows the transfer functions $T_{x'}^{(\pm)}$ and $T_{z'}^{(\pm)}$ for $\Delta = |J|/2$ and $s = 1$. Note that the two cases ($D^{(+)}$ and $D^{(-)}$) can be easily distinguished by the sign of the transverse transfer function $T_{x'}^{(+)}$ and $T_{x'}^{(-)}$ for short transfer times (cf. Fig. 1A). More specifically, for $J > 0$ the transfer function $T_{x'}^{(+)}(\tau)$ is positive and $T_{x'}^{(-)}(\tau)$ is negative, if $\tau < \min\{\frac{1}{\Delta}, \frac{2}{3|J|-\Delta}\}$ and if $\Delta < 3|J|$ (cf. Fig. 2A). Conversely, for $J < 0$ the transfer function $T_{x'}^{(+)}(\tau)$ is negative and $T_{x'}^{(-)}(\tau)$ is positive. In contrast, the longitudinal transfer functions $T_{z'}^{(\pm)}$ (cf. Fig. 1B) are both positive and can only be distinguished by the transfer frequency (cf. Eq. (19)). In the general case ($s \neq 1$), the sign of the transverse transfer function for short mixing times does not directly reflect the sign of C_L. For $s > 0$ and $J > 0$ this is only the case if

$$\frac{1-s}{s} < \frac{\Delta}{|J|} < \frac{s+2}{s}. \tag{20}$$

For example, for $J = 7\,\mathrm{Hz}$ and a scaling factor $s = 0.8$ (corresponding to a typical MOCCA-M16 sequence [7]), the sign of the crosspeaks directly reflects the sign of $C_L = D + J$, if $2\,\mathrm{Hz} < \Delta < 25\,\mathrm{Hz}$. From the experimental point of view, it is interesting to study which transfer functions (longitudinal or transverse) are most suitable to distinguish the two possible dipolar coupling constants $D^{(+)}$ and $D^{(-)}$. For $s = 1$, $s = 0.5$, $s = 0.25$, and $s = -0.5$ [5], the difference $T_{x'}^{(+)} - T_{x'}^{(-)}$ between the transverse transfer functions is shown in Figs. 3A–D and the difference $T_{z'}^{(+)} - T_{z'}^{(-)}$ between the longitudinal transfer functions is shown in Figs. 3A′–D′ as a function of the mixing time τ for the splittings $0 \leqslant \Delta \leqslant 3|J|$.

Fig. 4 shows the root mean square difference

Table 1
Coupling parameters of the prepared cytosine samples

Sample	$Q(D_2O)$ (Hz)	J (Hz)	D (Hz)	$J + D$ (Hz)	D/J (Hz)
1	0	7.2	0	7.2	0
2	4.2	7.2	−4	3.2	−0.89
3	13.5	7.2	−10.7	−3.5	−3.29
4	18.8	7.2	−14.6	−7.4	−6.21

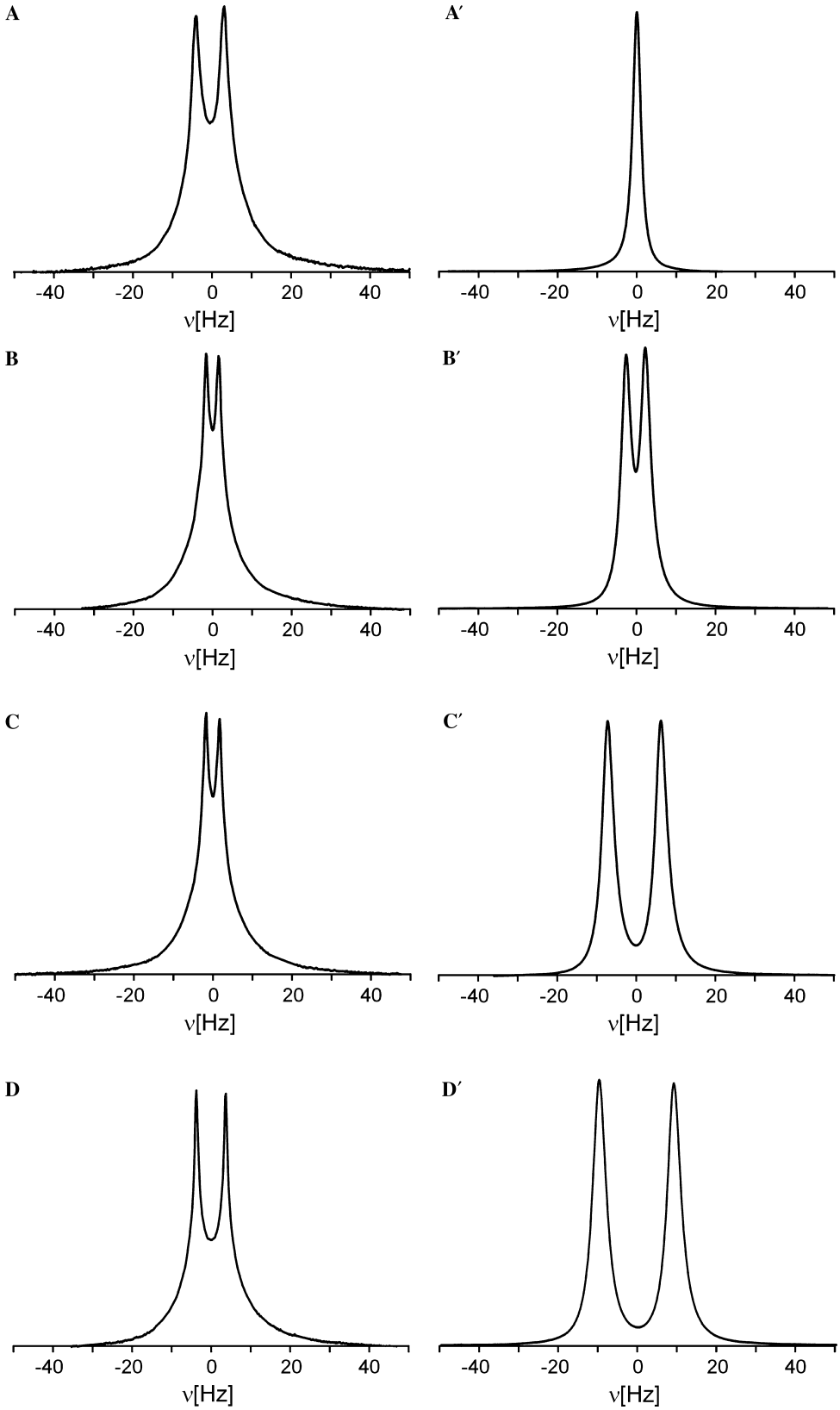

Fig. 5. Doublet splittings $\Delta = |D + J|$ of the H6 resonance of cytosine (A–D) and the corresponding residual deuterium quadrupolar splittings of D_2O (A′–D′) of four sample preparations with $\Delta \approx 7$ Hz (A and D) and $\Delta \approx 3.5$ (B and C) for sample 1 (A, A′), sample 2 (B, B′), sample 3 (C, C′), and sample 4 (D, D′) (see Table 1). The non-Lorentzian lineshapes are due to shimming problems.

$$q^{\mathrm{rms}} = \sqrt{\overline{\left(T_{\alpha'}^{(+)} - T_{\alpha'}^{(-)}\right)^2}} \tag{21}$$

between $T_{\alpha'}^{(+)}$ and $T_{\alpha'}^{(-)}$ for $\alpha' = \{x', y', z'\}$ and $0 \leqslant \tau \leqslant 1/J$. For positive scaling factors s, this rms difference is in general larger for transverse transfer functions if the splitting Δ is smaller than 3 J, i.e., transverse transfer functions $T_{x'}$ are preferable to solve the sign problem.

3. Experiments

To test this approach in practice, experimental coherence and polarisation transfer functions between H5 and H6 of cytosine were recorded in isotropic and anisotropic solutions. We prepared four samples with (see Table 1 and Fig. 5)

$D + J \approx \pm 3.5\,\mathrm{Hz}$ and $D + J \approx \pm 7\,\mathrm{Hz}$

by adjusting the concentration of commercially available phages (PF1-LP11-92, ASLA, Latvia) [5]. The residual quadrupolar splittings Q of the D_2O signal are summarized in Table 1 together with the experimentally determined isotropic (J) and dipolar (D) coupling constants, $C_L = D + J$ and the ratios D/J. In Fig. 5 the experimentally observed doublet of the H6 resonance with the splitting $\Delta = |D + J|$ and the corresponding deuterium doublet of the D_2O signal with the residual quadrupolar splitting Q are shown for all four samples.

After selective excitation of the H5 resonance, the experimental transfer functions were derived from the integrated intensity of the H6 resonance as a function of the TOCSY mixing time [5] for several TOCSY sequences with different dipolar scaling factors. The experimental and simulated transfer functions $T_{x'}^{(\pm)}$ and $T_{z'}^{(\pm)}$ for cytosine are shown in Fig. 6 for $|D + J| \approx 3.5$ Hz and in Fig. 7 for $|D + J| \approx 7\,\mathrm{Hz}$. The best match

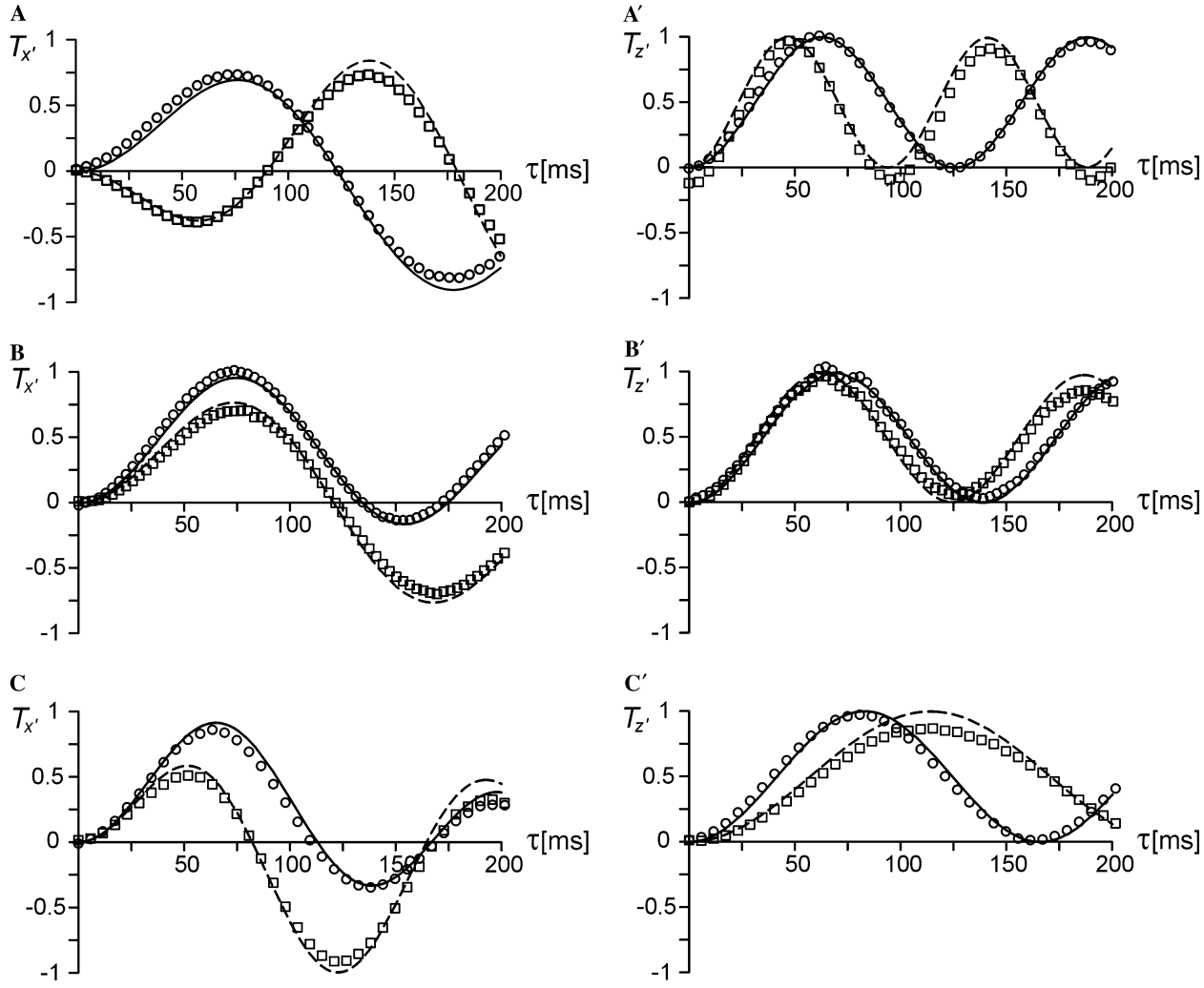

Fig. 6. Experimental (circles: $J + D \approx 3.5\,\mathrm{Hz}$, squares: $J + D \approx -3.5\,\mathrm{Hz}$) and simulated (solid curve: $J + D \approx 3.5\,\mathrm{Hz}$, dashed curve: $J + D \approx -3.5\,\mathrm{Hz}$) transverse (A–C) and longitudinal (A′–C′) transfer functions for the transfer between H5 and H6 of cytosine. Pulse sequences: MOCCA-M16 with $s \approx 0.8$ (A) MOCCA-XY16 with $s = 0.85$ (A′), MLEV-17 with $s = 0.25$ (B), MLEV-16 with $s = 0.25$ (B′), and DIPSI-2 with $s = -0.5$ (C, C′).

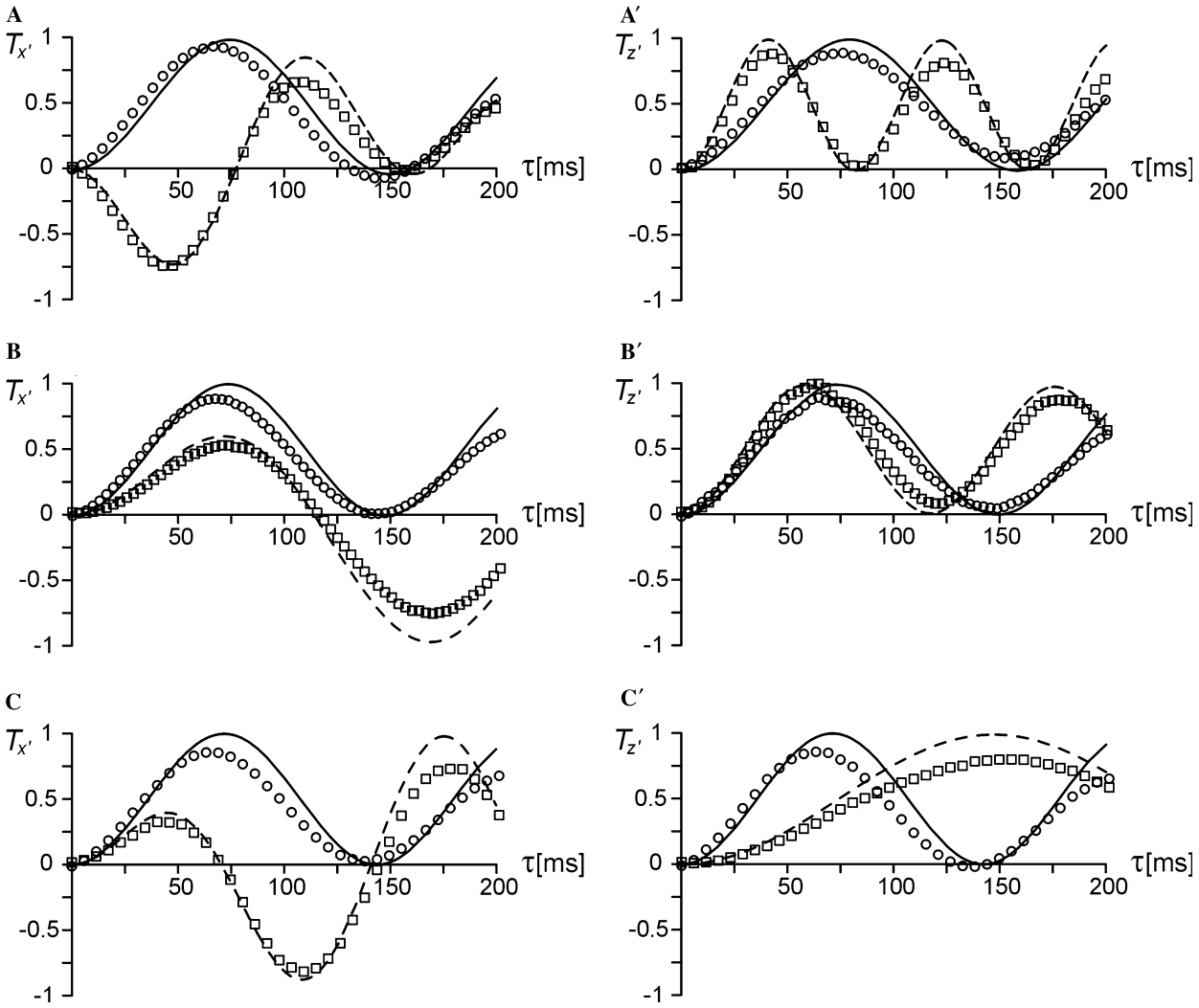

Fig. 7. Experimental (circles: $J + D \approx 7$ Hz, squares: $J + D \approx -7$ Hz) and simulated (solid curve: $J + D \approx 7$ Hz, dashed curve: $J + D \approx -7$ Hz) transverse (A–C) and longitudinal (A′–C′) transfer functions for the transfer between H5 and H6 of cytosine. Pulse sequences: MOCCA-M16 with $s \approx 0.8$ (A), MOCCA-XY16 with $s = 0.85$ (A′), MLEV-17 with $s = 0.25$ (B), MLEV-16 with $s = 0.25$ (B′), and DIPSI-2 with $s = -0.5$ (C, C′).

between simulated and experimental transfer functions was found for the scalar and dipolar coupling constants summarized in Table 1. A reasonable match is found between experimental and theoretical transfer functions. As expected, the sign of $C_L = D + J$ can be determined in Fig. 6A directly from the sign of the transverse transfer functions acquired with MOCCA-M16 with a dipolar scaling factor $s \approx 0.8$. The dipolar scaling factors of MOCCA-XY16, MLEV-16, and DIPSI-2 are $s = 0.85$, $s = 0.25$, and $s = -0.5$, respectively [5]. The longitudinal transfer functions (Figs. 6A′–C′) are always positive (cf. Eqs. (14) and (16)) and the sign of $C_L = D + J$ can only be distinguished for longer mixing times. In contrast, the sign of $C_L = D + J$ can directly be determined by the sign of the transverse MOCCA transfer function (Fig. 6A) for short mixing times. This may be an advantage in applications where relaxation losses cannot be neglected.

The experimental results in Figs. 6 and 7 show, that in the case of transverse magnetisation transfer with MOCCA-M16 the sign of the first extremum in the mixing time range from $\tau = 0$ to 100 ms is identical to the sign of $D + J$. Hence, for a typical J coupling of 7 Hz, a two-dimensional MOCCA-M16 experiment with a mixing time of 50 ms would allow us to determine the sign of $C_L = D + J$ simply based on the sign of the crosspeaks for a splitting between $0.25|J|$ and $3.5|J|$ for $s = 0.8$ (cf. Eq. (20)). So far, the discussion was restricted to the on-resonance case ($v_1 \approx v_2 \approx 0$). However, the results qualitatively also apply for offsets v_1 and v_2 that are within the active bandwidth of MOCCA-M16, which is in the order of the rms pulse amplitude [7]. This is demonstrated in Fig. 8, which shows the simulated crosspeak sign and amplitude for $J = 7$ Hz and residual dipolar coupling constants between 0 Hz (Fig. 8A) and −14 Hz (Fig. 8F) at a mixing time of 50 ms

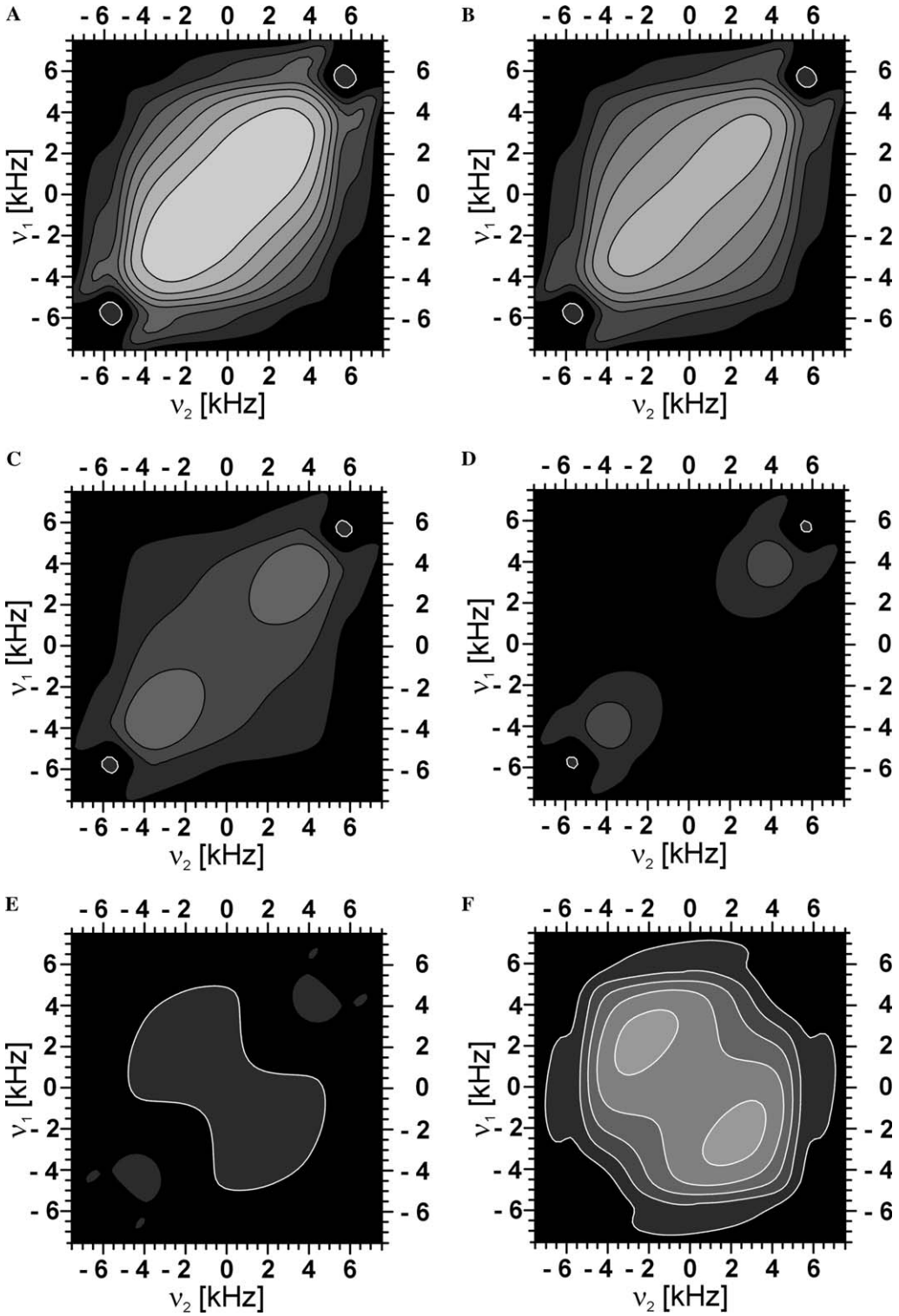

Fig. 8. Offset dependence of the transfer efficiency $T_y^{\mathrm{inh}}(v_1, v_2)$ under the MOCCA-M16 sequence with a dipolar scaling factor $s = 0.78$ at a mixing time $\tau_{\mathrm{mix}} = 50$ ms. The scalar coupling constant is $J = 7$ Hz and the dipolar coupling constants are (A) $D = 0$ Hz, (B) $D = -3.5$ Hz, (C) $D = -7$ Hz, (D) $D = -9$ Hz, (E) $D = -10.5$ Hz, and (F) $D = -14$ Hz. The sequence was normalized to an rms RF amplitude $v_{\mathrm{RF}}^{\mathrm{rms}} = 10$ kHz. To simulate the effects of RF inhomogeneity, a Gaussian RF inhomogeneity distribution with a full width at half maximum of 10% was assumed. Contour lines (black if positive, white if negative) are shown for $\pm 0.1, \pm 0.2, \ldots, \pm 0.9$. Areas with the same value of $|T_y^{\mathrm{inh}}|$ are filled with the same grey level (e.g., black for $|T_y^{\mathrm{inh}}| \leqslant 0.1$).

with $v_{\mathrm{rms}} = 10$ kHz. As expected for $\Delta > 0.25|J| \approx 2$ Hz (Figs. 8A, B and E, F), the sign of the crosspeak reflects the sign of $D + J$.

Remember that the previous discussion is strictly valid only for 2-spin systems. For systems consisting of three spins 1/2, analytical transfer functions are

available [8]. In more complicated spin systems, the transfer functions can be simulated numerically [9]. A further complication arises in applications to large molecules, such as proteins, where crossrelaxation rates are comparable to scalar and dipolar coupling constants. Here, TOCSY transfer through scalar and dipolar couplings can be accompanied by significant NOE or ROE contributions [3,10–14]. In the case of transverse MOCCA-M16 transfer, for example, TOCSY crosspeaks can be superimposed by negative ROESY crosspeaks if two coupled spins are close in space. This effect must be taken into account when protein spectra are analysed. To show this phenomenon, here we present MOCCA-XY16-SIAM spectra [22] of basic pancreatic trypsin inhibitor (BPTI). Partial alignment of the protein molecules was achieved by the addition of 12 wt% lipid bicelles [20,21]. The H_N–H_α crosspeak amplitudes were carefully analysed for Asp 3 and Phe 45. For the scalar and residual dipolar coupling constants of Asp 3 and Phe 45 (cf. Table 2), the H_N–H_α crosspeak intensities were simulated numerically [9] as a function of the MOCCA-M16 mixing period (see Fig. 9). In the simulation, the experimental offsets of the spins (cf. Table 3) and the effects of RF inhomogeneity were taken into account, but crossrelaxation effects were not considered in the simulation. For a mixing period of 30 ms, both H_N–H_α crosspeaks are expected to be positive in the absence of ROE contributions. Note, however, the significantly larger amplitude of the simulated crosspeak of Phe 45 compared to Asp 3. The former crosspeak should, therefore, be less susceptible to the suspected ROE contributions. Indeed, the crosspeak of Phe 45 is positive

Table 2
Coupling parameters for the spin systems of Asp 3 and Phe 45 in aligned BPTI

Residue 1	Atom 1	Residue 2	Atom 2	J (Hz)	D (Hz)
Asp 3					
Asp(3)	H_N	Asp(3)	H_α	6.8	3.1
Asp(3)	H_N	Pro(2)	H_α	0	16.3
Asp(3)	H_N	Asp(3)	$H_{\beta1}$	0	13.4
Asp(3)	H_N	Asp(3)	$H_{\beta2}$	0	4.7
Asp(3)	H_α	Pro(2)	H_α	0	2.4
Asp(3)	H_α	Asp(3)	$H_{\beta1}$	6.6	−1.7
Asp(3)	H_α	Asp(3)	$H_{\beta2}$	6.6	3.3
Asp(3)	$H_{\beta1}$	Asp(3)	$H_{\beta2}$	13	23.9
Asp(3)	$H_{\beta1}$	Pro(2)	H_α	0	1.9
Asp(3)	$H_{\beta2}$	Asp(2)	H_α	0	1.1
Phe 45					
Phe(45)	H_N	Phe(45)	H_α	10.2	5.1
Phe(45)	H_N	Asn(44)	H_α	0	8.2
Phe(45)	H_N	Phe(45)	$H_{\beta1}$	0	7.3
Phe(45)	H_N	Phe(45)	$H_{\beta2}$	0	3.4
Phe(45)	H_α	Asn(44)	H_α	0	2.6
Phe(45)	H_α	Phe(45)	$H_{\beta1}$	6.6	0.9
Phe(45)	H_α	Phe(45)	$H_{\beta2}$	6.6	5.5
Phe(45)	$H_{\beta1}$	Phe(45)	$H_{\beta2}$	13	26.6
Phe(45)	$H_{\beta1}$	Asn(44)	H_α	0	1.5
Phe(45)	$H_{\beta2}$	Asn(44)	H_α	0	1.1

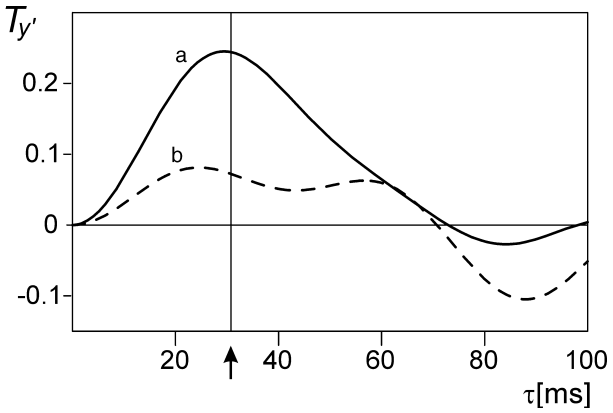

Fig. 9. Numerical simulations of the transfer of y-magnetisation under MOCCA-M16 with an RF power (corresponding to the root mean square RF amplitude) $\nu_{RF}^{rms} \approx 7$ kHz in two 5-spin systems (cf. Tables 2 and 3) neglecting relaxation effects. (a) H_N (Phe 45) $\rightarrow H_\alpha$ (Phe 45) for spin system 2 and (b) H_N (Asp 3) $\rightarrow H_\alpha$ (Asp 3) for spin system 1. Transfer efficiency after $\tau_{mix} = 30.78$ ms (see arrow): (a) 0.24 and (b) 0.07. For the simulations of the effects of RF inhomogeneity a Gaussian RF inhomogeneity distribution with a full width at half maximum of 10% was assumed.

Table 3
Offsets for the spin systems of Asp 3 and Phe 45 in aligned BPTI

Residue	Atom	Offset (Hz)
Asp 3		
Asp(3)	H_N	1059
Asp(3)	H_α	−1151
Asp(3)	$H_{\beta1}$	−1891
Asp(3)	$H_{\beta2}$	−1891
Pro(2)	H_α	−1111
Phe 45		
Phe(45)	H_N	1690
Phe(45)	H_α	−711
Phe(45)	$H_{\beta1}$	−1576
Phe(45)	$H_{\beta2}$	−1886
Asn(44)	H_α	−831

in the experimental 2D spectrum (see Fig. 10). In contrast, a negative crosspeak is found for Asp 3 which must be ascribed to the influence of the discussed ROE contributions. It is, furthermore, interesting to note that the crosspeaks due to a pure interresidual dipolar coupling, i.e., for $J = 0$ are usually negative as it is expected for $\Delta\tau < 1$ (see Eq. (18)). One example for such a negative transfer, the crosspeak between H_α of Ile 18 and H_N of Ile 19 is indicated in Fig. 10 (denoted by 18/19).

4. Conclusion

Conventional methods to define the relative sign and size of scalar and residual dipolar coupling constants between two spins require the presence of an additional spin [1]. Here, we demonstrate that the different forms of

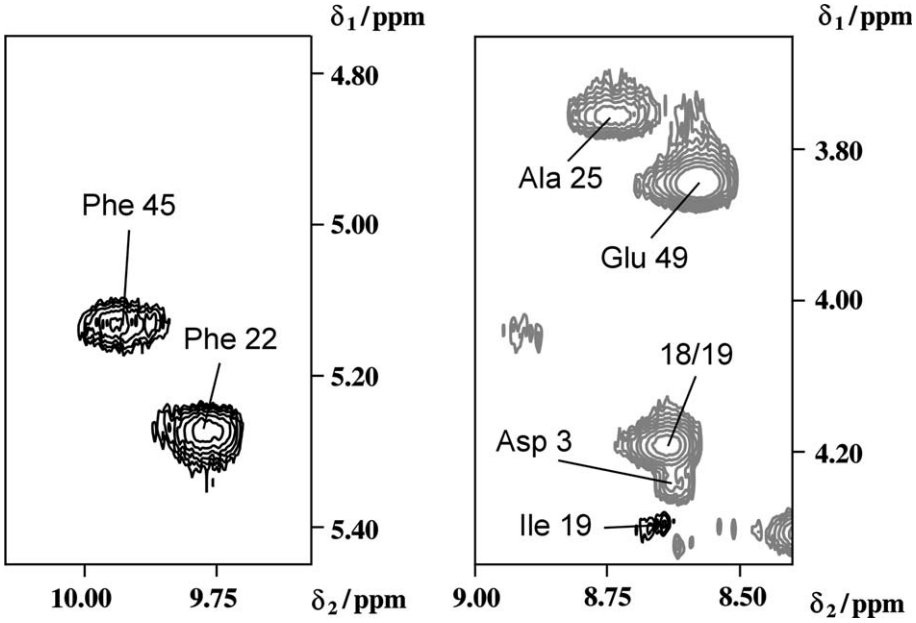

Fig. 10. Characteristic sections of a homonuclear 2D MOCCA-XY16-SIAM spectrum of BPTI measured in a magnetically oriented anisotropic solution containing 12 wt% lipid bicelles. The in-phase component of the spectrum is shown (for experimental details see [22]). Black contour lines: signals with positive transfer. Grey contour lines: signals with negative transfer.

scalar and residual dipolar coupling tensors make it possible to determine the relative sign and size of the coupling constants even for a simple homonuclear two-spin system (but not for heteronuclear spin systems). As shown analytically and experimentally for a model system, transverse transfer functions of TOCSY sequences such as MOCCA-M16 with a large dipolar scaling factor s (cf. Eq. (13)) are best suited to determine the relative sign and size of scalar and dipolar couplings. We also discussed potential problems created in spin systems consisting of more than two coupled spins and in applications to large molecules, where NOE and ROE contributions cannot be neglected. The first problem can be solved using numerical simulations but a possible experimental solution could be the use of band-selective TACSY sequences [3,15–18], which can reduce complicated coupling topologies to effective two-spin systems [3]. A possible experimental solution of the second problem could be the use of "clean" TOCSY experiments that are suitable for scalar and dipolar transfer [19].

References

[1] T. Carlomagno, W. Peti, C. Griesinger, A new method for the simultaneous measurement of magnitude and sign of $^1D_{CH}$ and $^1D_{HH}$ dipolar couplings in methylene groups, J. Biomol. NMR 17 (2000) 99–109.

[2] L. Braunschweiler, R.R. Ernst, Coherence transfer by isotropic mixing: application to proton correlation spectroscopy, J. Magn. Reson. 53 (1983) 521–528.

[3] S.J. Glaser, J.J. Quant, Homonuclear and heteronuclear Hartmann–Hahn transfer in isotropic liquids, in: W.S. Warren (Ed.), Advances in Magnetic and Optical Resonance, vol. 19, Academic Press, San Diego, 1996, pp. 59–252.

[4] M.R. Hansen, M. Rance, A. Pardi, Observation of long-range ^{1}H–^{1}H distances in solution by dipolar coupling interactions, J. Am. Chem. Soc . 120 (1998) 11210–11211.

[5] F. Kramer, S.J. Glaser, Efficiency of homonuclear Hartmann–Hahn and COSY-type mixing sequences in the presence of scalar and residual dipolar couplings, J. Magn. Reson. 155 (2002) 83–91.

[6] F. Kramer, B. Luy, S.J. Glaser, Offset dependence of homonuclear Hartmann–Hahn transfer based on residual dipolar couplings in solution state NMR, Appl. Magn. Reson. 17 (1999) 173–187.

[7] F. Kramer, W. Peti, C. Griesinger, S.J. Glaser, Optimized homonuclear Carr–Purcell-type dipolar mixing sequences, J. Magn. Reson. 149 (2001) 58–66.

[8] B. Luy, S.J. Glaser, Superposition of scalar and residual dipolar couplings: analytical transfer functions for three spins 1/2 under cylindrical mixing conditions, J. Magn. Reson. 148 (2001) 169–181.

[9] S.J. Glaser, G.P. Drobny, Assessment and optimization of pulse sequences for homonuclear isotropic mixing, in: W.S. Warren (Ed.), Advances in Magnetic and Optical Resonance, vol. 14, Academic Press, San Diego, 1990, pp. 35–58.

[10] C. Griesinger, G. Otting, K. Wüthrich, R.R. Ernst, Clean TOCSY for ^{1}H spin system identification in macromolecules, J. Am Chem. Soc. 110 (1988) 7870–7872.

[11] J. Briand, R.R. Ernst, Computer-optimized homonuclear TOCSY experiments with suppression of cross relaxation, Chem. Phys. Lett. 185 (1991) 276–285.

[12] J. Cavanagh, M. Rance, Suppression of cross-relaxation effects in TOCSY spectra via a modified DIPSI-2 mixing sequence, J. Magn. Reson. 96 (1992) 670–678.

[13] M. Kadkhodaei, T.-L. Hwang, J. Tang, A.J. Shaka, A simple windowless mixing sequence to suppress cross relaxation in TOCSY experiments, J. Magn. Reson. A 105 (1993) 104–107.

[14] U. Kerssebaum, R. Markert, J. Quant, W. Bermel, S.J. Glaser, C. Griesinger, Power reduction in clean TOCSY experiments with shaped pulses, J. Magn. Reson. 99 (1992) 185–191.

[15] S.J. Glaser, G.P. Drobny, The tailored TOCSY experiment: chemical shift selective coherence transfer, Chem. Phys. Lett. 164 (1989) 456–462.
[16] S.J. Glaser, Coupling topology dependence of polarization-transfer efficiency in TOCSY and TACSY experiments, J. Magn. Reson. A 104 (1993) 283–301.
[17] J. Quant, T. Prasch, S. Ihringer, S.J. Glaser, Tailored correlation spectroscopy for the enhancement of fingerprint cross peaks in peptides and proteins, J. Magn. Reson. B 106 (1995) 116–121.
[18] T. Carlomagno, T. Prasch, S.J. Glaser, COIN TACSY, a novel approach to tailored correlation spectroscopy, J. Magn. Reson. 149 (2001) 52–57.
[19] F. Kramer, S.J. Glaser, Clean TOCSY transfer through residual dipolar couplings, J. Magn. Reson. 2004 (in press).
[20] M. Ottiger, A. Bax, Characterization of magnetically oriented phospholipid micelles for measurement of dipolar couplings in macromolecules, J. Biomol. NMR 12 (1998) 361–372.
[21] J.A. Losonczi, J.H. Prestegard, Improved dilute bicelle solutions for high-resolution NMR of biological macromolecules, J. Biomol. NMR 12 (1998) 447–451.
[22] A. Möglich, M. Wenzler, F. Kramer, S.J. Glaser, E. Brunner, Determination of residual dipolar couplings in homonuclear MOCCA-SIAM experiments, J. Biomol. NMR 23 (2002) 211–219.